Molecular Brain

MICRO REPORT

Open Access

Electrophysiological characterization of a $Ca_V3.2$ calcium channel missense variant associated with epilepsy and hearing loss

Robin N. Stringer[1,2†], Leos Cmarko[2,3,4†], Gerald W. Zamponi[5], Michel De Waard[4] and Norbert Weiss[1*]

Abstract

T-type calcium channelopathies encompass a group of human disorders either caused or exacerbated by mutations in the genes encoding different T-type calcium channels. Recently, a new heterozygous missense mutation in the *CACNA1H* gene that encodes the $Ca_V3.2$ T-type calcium channel was reported in a patient presenting with epilepsy and hearing loss—apparently the first *CACNA1H* mutation to be associated with a sensorineural hearing condition. This mutation leads to the substitution of an arginine at position 132 with a histidine (R132H) in the proximal extracellular end of the second transmembrane helix of $Ca_V3.2$. In this study, we report the electrophysiological characterization of this new variant using whole-cell patch clamp recordings in tsA-201 cells. Our data reveal minor gating alterations of the channel evidenced by a mild increase of the T-type current density and slower recovery from inactivation, as well as an enhanced sensitivity of the channel to external pH change. To what extend these biophysical changes and pH sensitivity alterations induced by the R132H mutation contribute to the observed pathogenicity remains an open question that will necessitate the analysis of additional *CACNA1H* variants associated with the same pathologies.

Keywords Ion channels, Calcium channels, T-type channels, *CACNA1H*, $Ca_V3.2$, Mutation, Epilepsy, Hearing, Channelopathy

Mutations in the *CACNA1H* gene that encodes the $Ca_V3.2$ T-type calcium channel are risk factors for a number of human channelopathies including epilepsy [1], primary aldosteronism [2], autism spectrum disorder [3, 4], amyotrophic lateral sclerosis [5, 6], congenital amyotrophy [7], and trigeminal neuralgia [8, 9]. Recently, Algahtani and colleagues reported a new heterozygous missense mutation in a 50-year-old female patient with a clinical condition involving epilepsy and hearing loss which appears to be the first *CACNA1H* variant to be associated with sensorineural hearing alterations [10]. This mutation results in the substitution of an arginine at position 132 with a histidine (R132H) in the proximal extracellular end of the second transmembrane helix of $Ca_V3.2$ (Fig. 1a) and has not yet been reported in the gnomAD database (https://gnomad.broadinstitute.org/).

†Robin N. Stringer and Leos Cmarko contributed equally to this work.

*Correspondence:
Norbert Weiss
nalweiss@gmail.com
[1] Department of Pathophysiology, Third Faculty of Medicine, Charles University, Prague, Czech Republic
[2] Institute of Organic Chemistry and Biochemistry, Czech Academy of Sciences, Prague, Czech Republic
[3] Institute of Biology and Medical Genetics, First Faculty of Medicine, Charles University, Prague, Czech Republic
[4] Nantes Université, CNRS, INSERM, l'Institut du Thorax, Nantes, France
[5] Department of Clinical Neurosciences, Alberta Children's Hospital Research Institute, Hotchkiss Brain Institute, Cumming School of Medicine, University of Calgary, Calgary, Canada

Molecular simulation using the AlphaFold-generated model of the human $Ca_v3.2$ channel shows that replacement of the arginine 132 with a histidine leads to an additional hydrogen bond with methionine 119 of the first transmembrane helix (Fig. 1a) that has the potential to alter the gating of the channel. In addition, a histidine residue has a highly variable pKa value depending of its direct environment indicating that its charge may vary subtly as a function of external pH. To challenge this hypothesis, we assessed the functional impact of the R132H variant on the biophysical properties of $Ca_v3.2$ using patch-clamp recordings in tsA-201 cells bathed in 5 mM barium as the charge carrier (see Additional file 1). Both cells expressing $Ca_v3.2$ wild-type (WT) and R132H mutant channels displayed characteristic low-voltage activated T-type currents (Fig. 1a, b). A significant 40% ($p=0.0285$) increase of the maximal macroscopic T-type conductance (G_{max}) was observed in cells expressing the R132H channel variant (0.52 ± 0.06 nS/pF, n = 26) compared to cells expressing the WT channel (0.37 ± 0.03 nS/pF, n = 24) (Fig. 1d) without any alteration of the voltage dependence of activation (Fig. 1e) or steady-state inactivation (Fig. 1f). An additional significant ($p=0.0342$) slowing of the time constant (τ) of recovery from inactivation was observed for R132H channels (467 ± 21 ms, n = 18) compared to WT channels (284 ± 34 ms, n = 10) (Fig. 1g) while fast activation and inactivation kinetics of the current remained unaltered (Fig. 1h).

Next, we aimed to assess the effect of extracellular pH (pH_e) on the regulation of the channels. Indeed, histidine residues theoretically bear a partial charge at physiological pH, although this is largely influenced by the direct environment of the residue, and therefore act as $[H^+]$ sensor as a result of protonation. Protonation may in turn mediate modulatory effects on voltage-gated channels, including $Ca_v3.2$ [11]. Given that the R132H variant implicates the introduction of histidine within the extracellular end of the second transmembrane helix of $Ca_v3.2$, we assessed the effects of extracellular pH changes, alkalization (pH_e 8.0) and acidification (pH_e 6.5), on T-type currents. Consistent with previous results on T-type channels [11, 12], extracellular alkalization and acidification produced a significant increase and decrease of the T-type current, respectively, in both $Ca_v3.2$ WT- and R132H-expressing cells (Fig. 1i, top panels). However, these effects were emphasized on $Ca_v3.2$ R132H-mediated currents. For instance, alkalization-mediated increase of the T-type current was 82% higher ($p=0.0176$) in cells expressing the R132H channel ($24.0 \pm 3.5\%$ increase, n = 23) compared to cells expressing the WT channel ($13.1 \pm 1.2\%$ increase, n = 16), whereas acidification-mediated decrease of the current was enhanced by 37% greater ($p=0.0087$) (from $-30.9 \pm 2.9\%$ decrease in WT, n = 15, to $-42.5 \pm 2.9\%$ for R132H, n = 19) (Fig. 1i, bottom panels). In addition, extracellular alkalization produced an acceleration of the kinetics of current activation and inactivation, whereas acidification produced the exact opposite (Fig. 1j, k, top panels). However, these effects were proportionally similar between WT and R132H channels (Fig. 1j, k, bottom panels).

Previous studies in animal models have documented the importance of T-type channels in the functioning of the auditory system. For instance, $Ca_v3.2$ channels are highly expressed in mouse spiral ganglion neurons (SGN) where they are necessary for spatiotemporal auditory processing [13]. However, they also exhibit age-dependent increases in expression levels that are causally associated with SGN degeneration, whereas T-type channel

(See figure on next page.)

Fig. 1 Functional properties of the $Ca_v3.2$ R132H variant associated with epilepsy and hearing loss. **a** AlphaFold model of the human $Ca_v3.2$ channel showing the location of the R132H mutation (left panel). In this model, the arginine (R) 132 is located within the extracellular-exposed proximal end of the second transmembrane helix (S2) of $Ca_v3.2$ and forms two intra-helix hydrogen bonds with serine (S) 130 and leucine (L) 136 (left panel). Substitution of the R132 with a histidine (H) residue creates an additional hydrogen bond with methionine (M) 119 located within the first transmembrane helix (S1) of the channel. **b** Representative sets of whole-cell T-type current traces recorded in tsA-201 cells expressing $Ca_v3.2$ wild-type (WT) (black traces) and R132H variant (red traces). Currents were elicited by depolarizing steps to values ranging between − 90 mV and + 30 mV from a holding potential of − 100 mV. **c** Corresponding mean current/voltage (*I/V*) relationships. The continuous lines represent the fit of the *I/V* curves with the modified Boltzmann Eq. (1). **d** Corresponding mean maximal macroscopic conductance values (G_{max}) obtained from the fit of the *I/V* curves. **e** Corresponding mean normalized voltage dependence of activation fitted (continuous lines) with the modified Boltzmann Eq. (2). The inset shows the mean half-activation potential values obtained from the fit of the conductance curves. **f** Mean normalized voltage dependence of steady-state inactivation fitted with the two-state Boltzmann Eq. (3). The inset represents the mean half-inactivation potential values obtained from the fit of the inactivation curves. **g** Mean normalized recovery from inactivation kinetic fitted with the single-exponential function (4). Inset shows the mean time constant values obtained from the fit of the recovery from inactivation curves. **h** Mean time constant of fast activation (diamond symbols) and inactivation (round symbols) kinetics of T-type currents as a function of the membrane potential. **i** Relative change in peak current amplitude in response to extracellular pH alkalinization (pH_e 8.0, green symbols) and acidification (pH_e 6.5, orange symbols) from physiological pH_e 7.2 (top panels) as well as corresponding mean current change amplitude values (bottom panels). T-type currents were elicited by repetitive depolarizing steps to -20 mV from a holding potential of -100 mV. **j, k** Legend same as (**i**) but for T-type current activation and inactivation kinetics. Data are presented as mean ± S.E.M. and statistical analysis was performed using a two-tailed Student's *t* test

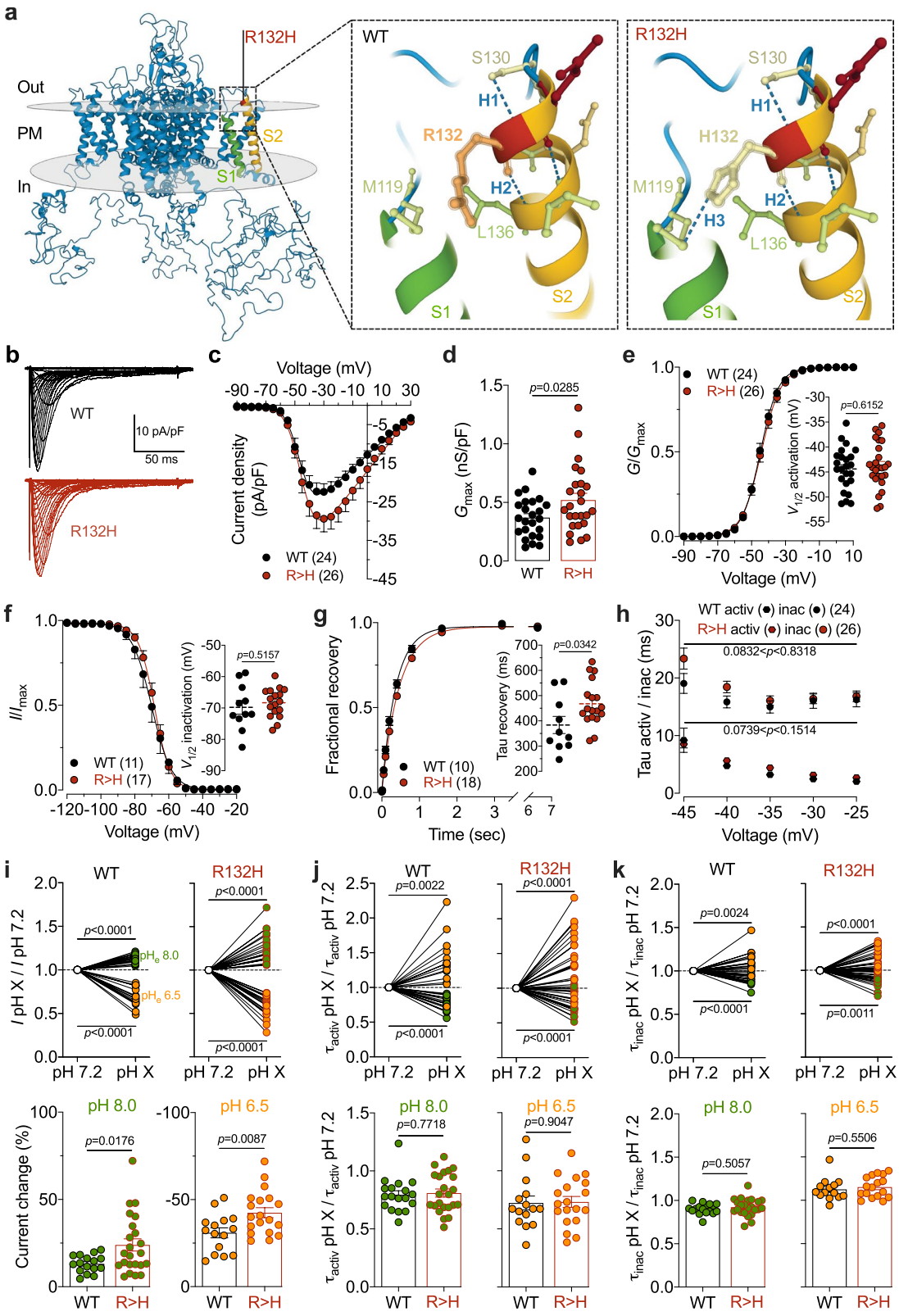

Fig. 1 (See legend on previous page.)

blockers are protective against age-related SGN and hearing loss [14]. Here, we showed that the $Ca_v3.2$ R132H mutation causes mixed alterations of the channel as evident from an increase in current density (that can be attributed to an alteration of the single channel gating properties and/or an increased expression of $Ca_v3.2$ at the cell surface) consistent with a gain-of-channel function. There is also a slowing of the recovery from inactivation which is consistent with a loss-of-function of the channel. However, the extent to which this loss-of-gating will manifest under physiological conditions will largely depend on the firing properties of nerve cells expressing the mutant channel. In addition, we illustrate that the R132H mutation enhances the impact of pH_e regulation of the channel. While the alterations may seem relatively mild, they have the merit to be observed and will require further experimentation to define their meaning in terms of pathogenicity. Clearly, there is evidence that alteration of pH homeostasis in response to primary metabolic disorders such as renal tubular acidosis is often accompanied with sensorineural hearing alterations [15]. In such context, altered pH_e-dependent modulation of $Ca_v3.2$ by the R132H mutation may represent a risk factor for hearing loss. Likewise, there is evidence that brain pH levels are significantly increased in experimental animal models of epilepsy [16–19] and patients [20] and precipitates the development of seizures. Therefore, it is a possibility that alkalinization-meditated increase of $Ca_v3.2$ R132H currents may also exacerbate seizures. An interesting consideration is whether a primary epilepsy could be the initiator of subsequent hearing loss in the patient carrying the $Ca_v3.2$ R132H mutation.

In conclusion, it is premature to recommend classifying the $Ca_v3.2$ R132H mutation as disease-causing variant at this stage in the absence of a larger number of variants causing the same pathologies. Moreover, since our functional analysis was performed in a recombinant expression system, there remains the possibility that the R132H mutation may exhibit a more pronounced phenotype in a native neuronal environment, and additional analysis will help to fully comprehend to which extent this mutation alters $Ca_v3.2$ channel function in the context of auditory function and epilepsy.

Abbreviations

Ca_v	Voltage-gated calcium channel
G_{max}	Maximal macroscopic conductance

Supplementary Information

The online version contains supplementary material available at https://doi.org/10.1186/s13041-023-01058-2.

Additional file 1. Supplementary material and methods.

Acknowledgements
Not applicable.

Author contributions
RNS and LC performed the electrophysiology and analyzed the data. NW designed and supervised the study. NW wrote the manuscript. GWZ and MDW edited the manuscript. All authors critically revised the manuscript and contributed significantly to this work. All authors read and approved the final manuscript.

Funding
L.C. is supported by a Barrande fellowship (Campus France). N.W. is supported by a Grant from the Czech Science Foundation (GACR #22-23242S) and the National Institute for Research of Metabolic and Cardiovascular Diseases (Program EXCELES # LX22NPO5104), funded by the European Union—Next Generation EU.

Availability of data and materials
All data generated or analyzed during this study are included in this published article and its additional files.

Declarations

Ethics approval and consent to participate
Not applicable.

Consent for publication
Not applicable.

Competing interests
The authors have no competing interests to declare.

Received: 14 August 2023 Accepted: 14 September 2023
Published online: 21 September 2023

References

1. Weiss N, Zamponi GW. Genetic T-type calcium channelopathies. J Med Genet. 2020;57(1):1–10.
2. Daniil G, Fernandes-Rosa FL, Chemin J, Blesneac I, Beltrand J, Polak M, et al. CACNA1H mutations are associated with different forms of primary aldosteronism. EBioMedicine. 2016;13:225–36.
3. Splawski I, Yoo DS, Stotz SC, Cherry A, Clapham DE, Keating MT. CACNA1H mutations in autism spectrum disorders. J Biol Chem. 2006;281(31):22085–91.
4. Viggiano M, D'Andrea T, Cameli C, Posar A, Visconti P, Scaduto MC, et al. Contribution of CACNA1H variants in autism spectrum disorder susceptibility. Front Psychiatry. 2022;13: 858238.
5. Rzhepetskyy Y, Lazniewska J, Blesneac I, Pamphlett R, Weiss N. CACNA1H missense mutations associated with amyotrophic lateral sclerosis alter Cav3.2 T-type calcium channel activity and reticular thalamic neuron firing. Channels (Austin). 2016;10(6):466–77.
6. Stringer RN, Jurkovicova-Tarabova B, Huang S, Haji-Ghassemi O, Idoux R, Liashenko A, et al. A rare CACNA1H variant associated with amyotrophic lateral sclerosis causes complete loss of Cav3.2 T-type channel activity. Mol Brain. 2020;13(1):33.
7. Carter MT, McMillan HJ, Tomin A, Weiss N. Compound heterozygous CACNA1H mutations associated with severe congenital amyotrophy. Channels (Austin). 2019;13(1):153–61.
8. Gambeta E, Gandini MA, Souza IA, Zamponi GW. CaV3.2 calcium channels contribute to trigeminal neuralgia. Pain. 2022;163:2315.
9. Mustafá ER, Gambeta E, Stringer RN, Souza IA, Zamponi GW, Weiss N. Electrophysiological and computational analysis of Cav3.2 channel variants associated with familial trigeminal neuralgia. Mol Brain. 2022;15(1):91.
10. Algahtani HA, Shirah BH, Samman A, Alhazmi A. Epilepsy and hearing loss in a patient with a rare heterozygous variant in the CACNA1H gene. J Epilepsy Res. 2022;12(1):33–5.

11. Delisle BP, Satin J. pH modification of human T-type calcium channel gating. Biophys J. 2000;78(4):1895–905.
12. Maksemous N, Blayney CD, Sutherland HG, Smith RA, Lea RA, Tran KN, et al. Investigation of CACNA1I Cav3.3 Dysfunction in Hemiplegic Migraine. Front Mol Neurosci. 2022;15:892820.
13. Lundt A, Seidel R, Soós J, Henseler C, Müller R, Bakki M, et al. Cav3.2 T-type calcium channels are physiologically mandatory for the auditory system. Neuroscience. 2019;409:81–100.
14. Lei D, Gao X, Perez P, Ohlemiller KK, Chen CC, Campbell KP, et al. Antiepileptic drugs delay age-related loss of spiral ganglion neurons via T-type calcium channel. Hear Res. 2011;278(1–2):106–12.
15. Ay E, Gurses E, Aslan F, Gulhan B, Alniacik A, Duzova A et al. Hearing loss related to gene mutations in distal renal tubular acidosis. Audiol Neurootol. 2023;1–10.
16. de Curtis M, Manfridi A, Biella G. Activity-dependent pH shifts and periodic recurrence of spontaneous interictal spikes in a model of focal epileptogenesis. J Neurosci. 1998;18:7543–51.
17. Schuchmann S, Schmitz D, Rivera C, Vanhatalo S, Salmen B, Mackie K, et al. Experimental febrile seizures are precipitated by a hyperthermia-induced respiratory alkalosis. Nat Med. 2006;12(7):817–23.
18. Helmy MM, Tolner EA, Vanhatalo S, Voipio J, Kaila K. Brain alkalosis causes birth asphyxia seizures, suggesting therapeutic strategy. Ann Neurol. 2011;69(3):493–500.
19. Lu D, Ji Y, Sundaram P, Traub RD, Guan Y, Zhou J, et al. Alkaline brain pH shift in rodent lithium-pilocarpine model of epilepsy with chronic seizures. Brain Res. 2021;1758: 147345.
20. Schuchmann S, Hauck S, Henning S, Grüters-Kieslich A, Vanhatalo S, Schmitz D, et al. Respiratory alkalosis in children with febrile seizures. Epilepsia. 2011;52(11):1949–55.

Publisher's Note